
EXPERIMENTAL STUDIES AT 6 - 12 GPa OF THE ONDERMATJIE HYPABYSSAL KIMBERLITE

Roger H. Mitchell

Department of Geology, Lakehead University Thunder Bay, Canada

INTRODUCTION

Despite many years of investigation the nature of the source rocks of kimberlite magma remains unidentified. In part, this is a consequence of the absence of rapidly-quenched lavas which might represent primary kimberlite magma. Typically kimberlites are hybrid rocks consisting of mantle-derived xenocrysts, cryptogenic macrocrysts and primary minerals. Commonly, their mineralogy and petrography indicates that their parental magmas have undergone flow differentiation and fractional crystallization. Samples of aphanitic kimberlite which are considered to represent the crystallization products of relatively unmodified magma have been the subjects of high pressure melting experiments in efforts to determine what rock types might represent their source rocks. In other approaches synthetic analogs of simplified bulk composition have been utilised. Other approaches are based purely upon geochemical arguments and arrive at very different conclusions. All of these studies are summarized by Mitchell (1995). Many experimental petrologists approach the problem by identifying liquidus phases at high pressure and assuming these are in equilibrium with source rocks. Another, less common, approach is to determine phase assemblages present over the whole melting interval and identify near-solidus assemblages representing potential source in metasomatized or veined mantle (Foley 1992).

This abstract summarise the results of a preliminary investigation of the phase relationships for a macrocryst- and xenocryst-poor, aphanitic hypabyssal kimberlite from Ondermatjie, Republic of South Africa. The bulk composition of this material is richer in titanium and total iron than the Wesselton aphanitic kimberlite previously studied experimentally at high pressure by Edgar & Charbonneau (1993). The kimberlite consists of microphenocrysts of forsteritic olivine set in a fine grained groundmass consisting principally of resorbed perovskite, subhedral magnesian ulvöspinel - magnetite, serphitic serpentine and

calcite. The whole rock composition (wt.%) is: 26.06 SiO₂; 4.04 TiO₂; 3.70 Al₂O₃; 14.38 Fe₂O₃; 0.18 MnO; 20.05 MgO; 16.58 CaO; 1.46 K₂O; 0.01 Na₂O; 0.84 P₂O₅; 0.09 Cr₂O₃; 11.58 LOI; 98.97 Total. The Clement contamination index of 1.30 indicates that this kimberlite can be considered as free of contamination by crustal rocks.

Experimental Techniques

All experiments were undertaken using the MA6/8 2000-ton uniaxial split-sphere multianvil apparatus located at the University of Alberta, Edmonton (Walter *et al.* 1995) at pressures ranging from 6 - 12 GPa and temperatures from 1000 - 1300°C. Starting material consisted of finely powdered kimberlite. Only the volatiles present in the starting composition were used in the experiments and no attempt was made to control oxygen fugacity. All experiments were conducted using either graphite (6 - 7 GPa) or platinum (8 - 12 GPa) capsules load into a furnace assembly consisting of a stepped graphite (6 - 7 GPa) or LaCrO₃ (8 - 12 GPa) heater contained within a semi-sintered MgO-Cr₂O₃ (5%) octahedron of either 18mm (6 - 7 GPa) or 14mm (8 - 12 GPa) edge length. Although none of the experiments were reversed the experimental approach of completely melting the starting material at 1600°C and then holding the charges at this temperature (~100- 200°C above the liquidus temperature) for 1-2 hours, followed by reducing the temperature to the desired experimental value is considered to result in a close approach to equilibrium. All temperatures were monitored with W5Re-W26Re thermocouples. Estimated temperature and pressures uncertainties are ± 10°C and ± 0.5GPa, respectively (Walter *et al.* 1995).

Experience with this equipment has demonstrated that at the temperatures and pressures prevailing equilibration tends to be rapid and is reached within the duration (8 hours) of the experiment.

Experimental charges were quenched to ambient conditions by first reducing temperature and then releasing pressure. Problems encountered in interpreting the experiments were: (1) the common occurrence of significant quenching effects on the phase assemblages present as represented by compositional zoning and heterogeneous inter-grain compositions, especially with respect to garnets; (2) phase segregation within the charges, with commonly one end of the capsule dominated by quenched carbonate liquid; (3) temperature gradients with the capsule, resulting in preferential crystallization of near-liquidus phases at one end of the capsule. Similar problems were encountered by Edgar & Charbonneau (1993) using this same apparatus. Regardless of these problems, observed phase assemblages are considered to be adequate for establishing the liquidus and subliquidus phase relationships.

All experimental products were examined by back-scattered electron imagery and the phases identified by energy dispersive X-ray spectrometry using a Hitachi 570 scanning electron microscope at Lakehead University. The compositions of phases were determined by quantitative energy dispersive X-ray spectrometry (EDS) using the LINK ISIS analytical system incorporating a Super ATWLightElement Detector (133 eV FWHM MnK). EDS spectra were acquired for 120 seconds (live time) with an accelerating voltage of 20 kV and beam current of 0.84 - 0.86 nA. Spectra were processed with the LINK-ISIS SEMQUANT software package with full ZAF corrections using well-characterized natural and synthetic standards.

Phase Relationships

Figure 1 illustrates liquidus and subliquidus phase relationships for this bulk composition as deduced from examination of the products of the experiments. All crystals in these products are newly-formed and not relicts of the starting material. The sub-liquidus region is divided into regions of phase assemblages representing the appearance of new phases as the melt cools. All of these lines, which should be regarded as approximate in their position, do not represent phase boundaries as they violate Schreinemakers rules; *e.g.* a four phase field is expected below the three phase olivine-garnet-liquid field rather than the observed five phase region.

The experiments indicate that the liquidus for this bulk composition rises steeply from about 1300°C at 5 GPa to about 1400°C at 10 GPa. This slope is similar to that determined by Edgar & Charbonneau (1993) for the Wesselt on aphanitic kimberlite but lies at much lower

temperatures (approx. 1560°C at 5 GPa; 1625°C at 10 GPa). The liquidus phase is olivine over the pressure range investigated (5-7 GPa) is forsteritic olivine. This is followed with decreasing temperature by the olivine plus garnet as the initial sub-liquidus solid phase assemblage. It can be expected that the olivine-only region will probably “wedge-out” with increasing pressure as olivine is replaced by olivine plus garnet as the liquidus phases. Garnets in the near-liquidus region are Ti-Ca-rich varieties (see below) belonging to the pyrope-grossular-almandine solid solution series (Dawson and Stephens’ group 6) and are thus compositionally-distinct from pyrope garnets of the megacryst/macrocryst suite (Dawson and Stephens’ groups 1 & 2). Notably absent as liquidus or near-liquidus phases are pyrope, orthopyroxene, and clinopyroxene.

Regardless of the differences in bulk composition the phase relationships established in these experiments are identical to those observed by Edgar & Charbonneau (1993), who also observed a wide three phase field of garnet + olivine + liquid as a near-liquidus phase assemblage. They differ in that the appearance of this assemblage occurred at much high temperatures; approx. 1475°C versus 1280°C (this work) at 6 GPa.

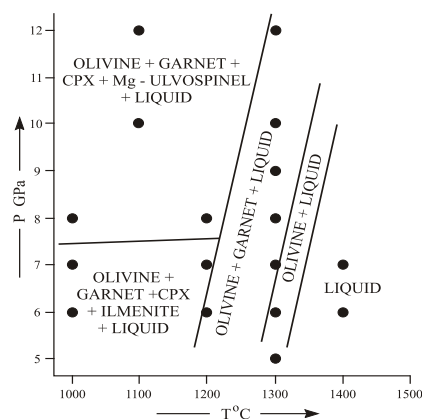


Figure 1. Phase relationships of Ondermatjie kimberlite

The absence of orthopyroxene, clinopyroxene and pyrope as near-liquidus phases in the experiments implies that, under the conditions used, liquid is not in equilibrium with a garnet lherzolite assemblage, and therefore this rock cannot be the source of kimberlite magmas.

In contrast to that of Edgar & Charbonneau (1993), this study extended the investigation to near-

solidus conditions (900 - 1000°C at 6 - 8 GPa). Figure 1 shows that supra-solidus assemblages consist of olivine+garnet+clinopyroxene+ilmenite (+/- perovskite)+liquid at 5-7 GPa or olivine+garnet+clinopyroxene+Mg-ulvospinel (+/- perovskite)+liquid at 8-12 GPa. These data suggest that primary clinopyroxene might have been found in the experiments of Edgar & Charbonneau (1993) at temperatures below 1300°C; the lowest they investigated. These data also indicate that kimberlite magmas are unlikely to be derived from simple garnet lherzolite sources.

Pyroxene-oxide Intergrowths.

One interesting, and unexpected, result of the experiments is the formation of orientated intergrowths between iron titanium oxides and silicates. The textures formed are identical to the lamellar intergrowths between magnesian ilmenite and clinopyroxene found in some megacrysts. The experimentally-formed oxide-silicate intergrowths occur between magnesium ilmenite and clinopyroxene at pressures less than 7.5 GPa, and between magnesian ulvospinel (qandilite) - ulvospinel solid solutions above this pressure. In addition intergrowths between spinel and olivine are also formed at 12 GPa. These intergrowths are considered not to result from exsolution of the oxide from a phase enriched in Ti, Mg and Fe. They undoubtedly represent a directionally-solidified intergrowth involving rapid crystallization at a (pseudo?)cotectic.

Ilmenites and clinopyroxenes in the intergrowths are similar in composition to those of the natural material (Table 1; Figs. 2 & 3). Spinel solid solutions in the intergrowths are dominated by the ulvospinel component (Table 2), and associated clinopyroxenes are Ca-rich relative to pyroxene associated with ilmenite (Fig. 2).

Garnets formed in the experiments exhibit a range in composition with respect to their Ti, Al, Mg, and Fe contents (Table 1). Many have Fe-enriched quench rims. There is no apparent relation between Ti content or Mg/Mg+Fe ratio and conditions of formation. They are unusual in that their overall composition is $(Ca,Mg)_3(Al,Fe,Ti,Cr)_2(Si_3O_{12})$ and are thus members of the grossular-pyrope-almandine solid solution series, and similar to eclogitic garnets rather than the pyrope garnets found in garnet lherzolites. Garnets of similar composition were formed in the experiments of Edgar & Charbonneau (1993).

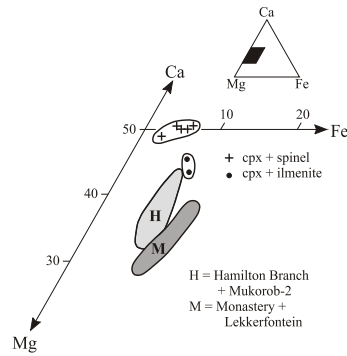


Figure 2. Compositions of clinopyroxenes in intergrowths.

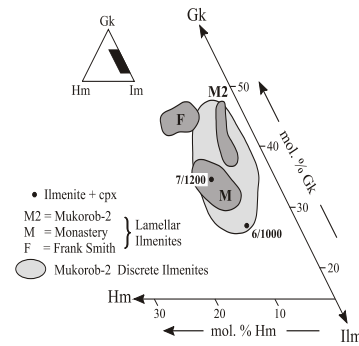


Figure 3 Compositions of ilmenite in intergrowths

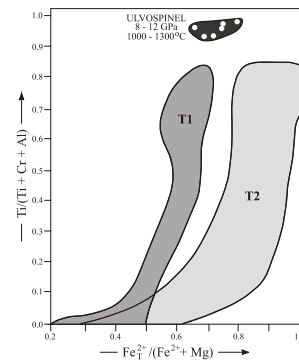


Figure 4 Compositions of spinel in intergrowths.

Quench Liquids are carbonates which exhibit a very wide range in composition. Those occurring in the mesostasis to primary and quench silicate assemblage are primarily dolomitic-to-magnesitic *e.g.* 40.7 wt.% MgO, 4.5 wt.% FeO; 2.7 wt.% CaO at 12 GPa/1300°C; 35.1 wt.% MgO, 2.2 wt.% CaO, 4.6 wt.% MgO at 8 GPa/1000°C; 9.7 wt.% MgO, 38.5 wt.% CaO, 1.76 wt.% FeO. Segregated quenched liquids are mixtures of cryptocrystalline silicate and dolomitic carbonate containing several wt.% K₂O (7.3 wt.% at 12 GPa/1300°C; 8.3 wt.% at 7 GPa/1400°C).

Conclusions The experimental data are interpreted to indicate that the crystallization sequence from liquidus to solidus of this bulk composition is: olivine; olivine + Ti-garnet; olivine + Ti-garnet + clinopyroxene + Fe-Ti-oxide. The subsolidus assemblage will probably consist of olivine-Ti-garnet - clinopyroxene - Fe-Ti-oxide - CaTiO₃ - magnesite-rich carbonate. The concentration of K in segregated liquids suggests that phlogopite might also occur. This assemblage is considered to exist as veins in a metasomatised asthenospheric mantle substrate.

REFERENCES:

- Edgar, A.D., Charbonneau, H.E. 1993. Melting experiments on a SiO₂-poor, CaO-rich aphanitic kimberlite from 5-10 GPa and their bearing on sources of kimberlite magmas. *American Mineralogist* 78, 132-142.
- Foley, S.F. 1992. Vein plus wall rock melting mechanisms in the lithosphere and the origin of potassic magmas. *Lithos* 28, 435-453.
- Mitchell, R.H. Kimberlites, 1995. Orangeites and Related Rocks. Plenum Press, New York.
- Walter, M.J., Thibault, Y., Wei, K., Luth, R.W. 1995. Characterizing experimental pressure and temperature conditions in multianvil apparatus. *Canadian Journal of Physics*, 73, 273-286.

Table 1. Composition (wt.%) of clinopyroxene in intergrowths and garnets

| P/T | 6/1000 | 7/1200 | 8/1000 | 8/1400 | 10/1100 | 6/1300 | 8/1400 |
|-------------------------------------|--------|--------|--------|--------|---------|--------|--------|
| SiO ₂ | 53.36 | 52.88 | 54.95 | 54.32 | 54.49 | 37.10 | 37.65 |
| TiO ₂ | 0.43 | 0.71 | 0.46 | 0.48 | 0.23 | 8.46 | 5.53 |
| Al ₂ O ₃ | 1.53 | 1.17 | 0.53 | 0.63 | 0.18 | 11.54 | 10.70 |
| Cr ₂ O ₃ | 0.11 | 0.14 | n.d. | n.d. | 0 | 0.10 | 0.14 |
| Fe ₂ O ₃ | 0 | 1.74 | 0 | 0 | 0.10 | - | - |
| FeO | 5.53 | 3.75 | 3.37 | 2.91 | 1.98 | 10.44 | 12.98 |
| MnO | n.d. | 0.25 | 0.13 | 0.10 | n.d. | 0.39 | 0.20 |
| MgO | 15.31 | 16.70 | 18.63 | 18.40 | 17.68 | 8.73 | 12.61 |
| CaO | 23.02 | 22.70 | 23.12 | 22.85 | 24.48 | 22.60 | 19.35 |
| Na ₂ O | n.d. | 0.22 | n.d. | n.d. | 0.11 | - | - |
| Total | 99.29 | 100.27 | 101.21 | 99.69 | 99.25 | 99.36 | 99.16 |
| <i>Mol. % End Member Components</i> | | | | | | | |
| CaTiAl ₂ O ₆ | 1.23 | 1.95 | 1.12 | 1.18 | 0.39 | | |
| CaAl(SiAl)O ₆ | 0.37 | 0 | 0 | 0 | 0 | | |
| Ac | 0 | 1.56 | 0 | 0 | 0.78 | | |
| Wo | 46.15 | 43.54 | 43.53 | 44.19 | 47.81 | | |
| Fs | 8.80 | 7.36 | 5.06 | 4.45 | 2.78 | | |
| En | 43.45 | 45.58 | 49.89 | 50.18 | 48.24 | | |
| Coexisting phase | ILM | ILM | SP | SP | SP | | |

Table 2. Compositions (wt.%) of ilmenite and spinels in intergrowths.

| P/T | 6/1000 | 7/1200 | | 8/1000 | 8/1300 | 10/1100 | 12/1100 |
|------------------------------------|--------|--------|----------------------------------|--------|--------|---------|---------|
| TiO ₂ | 49.33 | 50.76 | | 35.55 | 32.92 | 33.31 | 32.95 |
| Al ₂ O ₃ | 0.54 | 0.64 | | 0.95 | 1.48 | 0.44 | 0.52 |
| Cr ₂ O ₃ | 0.16 | 0.20 | | 0.16 | 0.25 | 0.23 | 0.05 |
| Fe ₂ O ₃ | 9.56 | 12.16 | | 0.10 | 7.99 | 5.70 | 8.11 |
| FeO | 30.92 | 27.77 | | 50.97 | 46.28 | 50.60 | 47.85 |
| MnO | 0.39 | 0.28 | | 0.10 | 0.22 | 0.22 | 0.56 |
| MgO | 7.32 | 9.87 | | 7.66 | 9.80 | 6.77 | 8.35 |
| | 98.22 | 101.68 | | 95.49 | 98.94 | 97.27 | 98.39 |
| <i>Mol.% End member components</i> | | | | | | | |
| Al ₂ O ₃ | 0.77 | 0.87 | MgAl ₂ O ₄ | 1.37 | 2.05 | 0.63 | 0.73 |
| Cr ₂ O ₃ | 0.15 | 0.18 | Mg ₂ TiO ₄ | 19.96 | 24.17 | 17.92 | 21.64 |
| Hm | 8.76 | 10.59 | MgCr ₂ O ₄ | 0 | 0 | 0 | 0 |
| Py | 0.80 | 0.55 | MnCr ₂ O ₄ | 0 | 0 | 0 | 0 |
| Gk | 26.57 | 34.06 | Mn ₂ TiO ₄ | 0.16 | 0.33 | 0.34 | 0.85 |
| Ilm | 62.94 | 53.74 | Fe ₂ TiO ₄ | 78.22 | 62.64 | 73.07 | 65.86 |
| | | | FeCr ₂ O ₄ | 0.16 | 0.23 | 0.22 | 0.05 |
| | | | Fe ₃ O ₄ | 0.13 | 10.59 | 7.82 | 10.88 |